Double handbag description of proton-antiproton annihilation into a heavy meson pair

A.T. Goritschnig[a 1], B. Pire[a 2], W. Schweiger[b 3]

a) *Centre de Physique Théorique, École Polytechnique, CNRS, 91128 Palaiseau, France*
b) *Institut für Physik, Karl-Franzens-Universität Graz, 8010 Graz, Austria*

Abstract

We propose to describe the process $p\bar{p} \to \overline{D^0} D^0$ in a perturbative QCD motivated framework where a double-handbag hard process $ud\bar{u}\bar{d} \to \bar{c}c$ factorizes from transition distribution amplitudes, which are quasi forward hadronic matrix elements of $\Psi_q \Psi_q \Psi_c$ operators, where q denotes light quarks and c denotes the heavy quark. We advocate that the charm-quark mass acts as the large scale allowing this factorization. We calculate this process in the simplified framework of the scalar diquark model and present the expected cross sections for the PANDA experiment at GSI-FAIR.

PACS: 13.75.-n, 25.43.+t, 13.85.Fb

1 Introduction

The collinear factorization framework allows to calculate a number of hard exclusive amplitudes in terms of perturbatively calculable coefficient functions and non-perturbative hadronic matrix elements of light-cone operators. The prime example is the calculation of the deeply virtual Compton-scattering (DVCS) amplitude in the handbag approximation with generalized parton distributions (GPDs), non-forward matrix elements of a quark-antiquark non local operator $\Psi(z)\overline{\Psi}(0)$ between an incoming and an outgoing baryon state. Strictly speaking, this description is only valid in a restricted kinematical region, called the generalized Bjorken scaling region, for a few specific reactions, and in the leading-twist approximation. It is, however, suggestive to extend this framework to the description of other reactions where the presence of a hard scale seems to justify the factorization of a short-distance dominated partonic subprocess from long-distance hadronic matrix elements. Such an extension has, in particular, been proposed in [1] for the reaction $p\bar{p} \to \Lambda_c \bar{\Lambda}_c$ with nucleon to charmed baryon GPDs. The extension of the collinear factorization framework to the backward region of DVCS and deep exclusive meson production [2, 3] leads to the definition of transition distribution amplitudes (TDAs) as non-forward matrix elements of a three-quark non-local operator $\Psi(z)\Psi(y)\Psi(0)$ between an incoming and an outgoing state carrying a different baryon number. Here too, this description

[1] Email:alexander.goritschnig@cpht.polytechnique.fr
[2] Email:bernard.pire@cpht.polytechnique.fr
[3] Email:wolfgang.schweiger@uni-graz.at

is likely to be valid in a restricted kinematical region, for a few specific reactions, and in the leading twist approximation. We propose here to extend the approach of [1] to the reaction $p\bar{p} \to \overline{D^0} D^0$ which will be measured with the PANDA [4] detector at GSI-FAIR. For this process the baryon number exchanged in the t-channel implies that hadronic matrix elements with $\Psi(z)\Psi(y)\Psi(0)$ operators enter the game. Let us stress that we have no proof of the validity of this approximation but take it as an assumption to be confronted with experimental data. For this approach to be testable, one needs to model the occurring nucleon to charmed meson TDAs. In contrast to the $N \to \pi$ TDAs, which have been much discussed [5], we do not have any soft meson limit to normalize these TDAs. We will rather use an overlap representation in the spirit of [6].

2 Hadron Kinematics

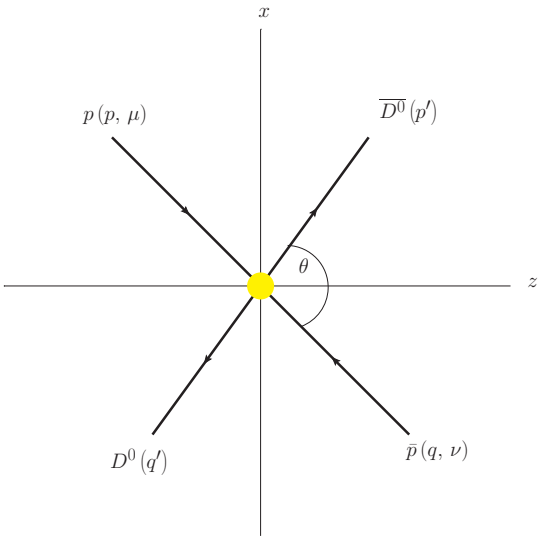

Figure 1: Kinematics of $p\bar{p} \to \overline{D^0} D^0$ in the symmetric CMS.

The kinematical situation for $p\bar{p} \to \overline{D^0} D^0$ scattering is sketched in Fig. 1. The momenta and helicities of the incoming proton and antiproton are denoted by p, μ and q, ν, the momenta of the outgoing $\overline{D^0}$ and D^0 by p' and q', respectively. The mass of the proton is denoted by m, that of the D^0 by M. We choose a symmetric center-of-momentum system (CMS) in which the longitudinal direction is defined by the average momentum of the incoming proton and the outgoing $\overline{D^0}$, respectively. The transverse momentum transfer is symmetrically shared between the incoming and outgoing hadrons.

In light-cone (LC) coordinates the hadronic momenta are parameterized as follows,

$$
\begin{aligned}
p &= \left[(1+\xi)\bar{p}^+, \frac{m^2+\boldsymbol{\Delta}_\perp^2/4}{2(1+\xi)\bar{p}^+}, -\frac{\boldsymbol{\Delta}_\perp}{2}\right], \quad p' = \left[(1-\xi)\bar{p}^+, \frac{M^2+\boldsymbol{\Delta}_\perp^2/4}{2(1-\xi)\bar{p}^+}, +\frac{\boldsymbol{\Delta}_\perp}{2}\right], \\
q &= \left[\frac{m^2+\boldsymbol{\Delta}_\perp^2/4}{2(1+\xi)\bar{p}^+}, (1+\xi)\bar{p}^+, +\frac{\boldsymbol{\Delta}_\perp}{2}\right], \quad q' = \left[\frac{M^2+\boldsymbol{\Delta}_\perp^2/4}{2(1-\xi)\bar{p}^+}, (1-\xi)\bar{p}^+, -\frac{\boldsymbol{\Delta}_\perp}{2}\right],
\end{aligned} \tag{1}
$$

where we have introduced sums and differences of the hadron momenta:

$$
\bar{p} := \frac{1}{2}(p+p'), \qquad \bar{q} := \frac{1}{2}(q+q') \qquad \text{and} \qquad \Delta := p'-p = q-q'. \tag{2}
$$

The minus momentum components can be obtained by using the on-mass shell conditions $p^2 = q^2 = m^2$ and $p'^2 = q'^2 = M^2$. The skewness parameter ξ gives the relative momentum transfer in the plus direction, i.e.

$$
\xi := \frac{p^+ - p'^+}{p^+ + p'^+} = -\frac{\Delta^+}{2\bar{p}^+}. \tag{3}
$$

The Mandelstam variable s is given by

$$
s = (p+q)^2 = \left(p'+q'\right)^2. \tag{4}
$$

In order to produce a $\overline{D^0}D^0$ pair, s must be larger than $4M^2$. The remaining Mandelstam variables, t and u, read:

$$
t = \Delta^2 = \left(p'-p\right)^2 = \left(q-q'\right)^2 \tag{5}
$$

and

$$
u = \left(q'-p\right)^2 = \left(p'-q\right)^2, \tag{6}
$$

so that $s+t+u = 2M^2+2m^2$. For later convenience we also introduce the abbreviations

$$
\Lambda_m := \sqrt{1-4m^2/s} \qquad \text{and} \qquad \Lambda_M := \sqrt{1-4M^2/s}. \tag{7}
$$

For further relations between the kinematical quantities see App. A.

3 Double Handbag Mechanism (DHM)

The double handbag mechanism (DHM) which we use to describe $p\bar{p} \to \overline{D^0}D^0$ is shown in Fig. 2. It is understood that the proton emits an $S[ud]$-diquark with momentum k_1 and the antiproton a $\overline{S[ud]}$-diquark with momentum k_2. They undergo a scattering with each other, i.e. they annihilate in our case into a gluon which subsequently decays into the heavy $\bar{c}c$ pair. Those produced heavy partons, characterized by k_1', λ_1' and k_2', λ_2', are re-absorbed by the remnants of the proton and the antiproton to form the $\overline{D^0}$ and the D^0, respectively. One could, of course, also think of vector-diquark configurations in the proton and $V[ud]\,\overline{V[ud]}$ annihilation to produce the

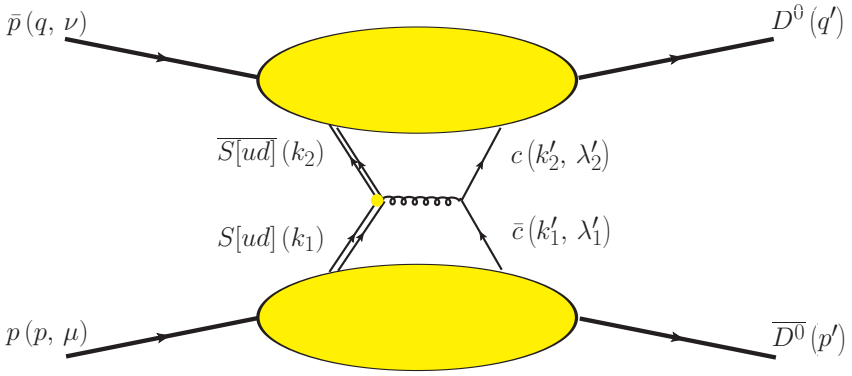

Figure 2: The handbag contribution to the process $p\bar{p} \to \overline{D^0} D^0$. The momenta and helicities of the baryons and quarks are specified.

$c\bar{c}$ pair. But in common diquark models of the proton it is usually assumed that the probability to find a $V\,[ud]$ diquark is smaller than the one for the $S\,[ud]$ diquark. Further suppression of $V\,[ud]$ diquarks as compared to $S\,[ud]$ diquarks occurs in hard processes via diquark form factors at the diquark-gluon vertices [7]. We thus expect that our final estimate of the $\overline{D^0} D^0$ cross section will not be drastically altered by the inclusion of vector-diquark contributions and we stick to the simpler scalar diquark model.

The whole hadronic four-momentum transfer Δ is also exchanged between the active partons in the partonic subprocess

$$S[ud](k_1)\,\overline{S[ud]}(k_2) \to \bar{c}(k_1', \lambda_1')\,c(k_2', \lambda_2')\,. \tag{8}$$

In (8) we neglect the mass of the $S[ud]-$(anti)diquark, but take into account the heavy (anti-) charm-quark mass m_c. In order to produce the heavy $\bar{c}c$ pair, the Mandelstam variable $\hat{s}$ of the partonic subprocess has to be

$$\hat{s} \geq 4m_c^2\,, \tag{9}$$

where $4m_c^2 \approx 6.5\,\mathrm{GeV}^2$. We have taken the (central) value for the charm-quark mass from the Particle Data Group [8], which gives $m_c = 1.275 \pm 0.025\,\mathrm{GeV}$. Thus the heavy-quark mass m_c is a natural intrinsic hard scale which demands that the intermediate gluon has to be highly virtual. This allows us to treat the partonic subprocess perturbatively, even at small $-t$, by evaluating the corresponding Feynman diagram. All the other non-active partons inside the parent hadrons are unaffected by the hard scattering and thus act as spectators.

For the double handbag mechanism the hadronic $p\bar{p} \to \overline{D^0}D^0$ amplitude can be written as

$$
\begin{aligned}
M_{\mu\nu} = & \sum_{a_i^{(\prime)}} \sum_{\alpha_i'} \int d^4\bar{k}_1 \theta(\bar{k}_1^+) \int \frac{d^4z_1}{(2\pi)^4} e^{i\bar{k}_1 z_1} \int d^4\bar{k}_2 \theta(\bar{k}_2^-) \int \frac{d^4z_2}{(2\pi)^4} e^{i\bar{k}_2 z_2} \\
& \times \langle \overline{D^0} : p' | \mathscr{T} \Psi^c_{a_1'\alpha_1'}(-z_1/2) \Phi^{S[ud]}_{a_1}(+z_1/2) | p : p, \mu \rangle \, \tilde{H}_{a_i^{(\prime)}\alpha_i'}(\bar{k}_1, \bar{k}_2) \\
& \times \langle D^0 : q' | \mathscr{T} \, \Phi^{S[ud]\dagger}_{a_2}(+z_2/2) \overline{\Psi}^c_{a_2'\alpha_2'}(-z_2/2) | \bar{p} : q, \nu \rangle \,,
\end{aligned}
\tag{10}
$$

where the assignment of momenta, helicities, etc. can be seen in Fig. 2. $a_i^{(\prime)}$ and α_i' denote color and spinor indices, respectively. In analogy to the hadronic level we have introduced the average partonic momenta $\bar{k}_i := (k_i + k_i')/2$, $i = 1, 2$, of the active partons. We note once more that the full hadronic momentum transfer is also transferred between the active partons, i.e. $k_1 - k_1' = p - p' = k_2' - k_2 = q' - q$.
The hard scattering kernel, denoted by $\tilde{H}_{a_i^{(\prime)}\alpha_i'}(\bar{k}_1, \bar{k}_2)$, describes the hard $S[ud]\overline{S[ud]} \to \bar{c}c$ subprocess. The soft part of the $p \to \overline{D^0}$ transition is encoded in the Fourier transform of a hadronic matrix element which is a time-ordered, bilocal product of a quark and a diquark field operator:

$$
\int \frac{d^4z_1}{(2\pi)^4} e^{i\bar{k}_1 z_1} \langle \overline{D^0} : p' | \mathscr{T} \Psi^c_{a_1'\alpha_1'}(-z_1/2) \Phi^{S[ud]}_{a_1}(+z_1/2) | p : p, \mu \rangle \,. \tag{11}
$$

In (11) $\Phi^{S[ud]}(+z_1/2)$ takes out an $S[ud]$-diquark from the proton state $|p : p, \mu\rangle$ at the space-time point $z_1/2$. The $S[ud]$ diquark then takes part in the hard partonic subproces. The $\Psi^c(-z_1/2)$ reinserts the $\bar{c}$-quark at $-z_1/2$ into the remnant of the proton which gives the desired final hadronic $\overline{D^0}$ state $|\overline{D^0} : p'\rangle$. At this stage the appropriate time-ordering of the quark field operators (denoted by the symbol $\mathscr{T}$) has to be taken into account. The remnant of the proton, which does not participate in the hard partonic subprocess, constitutes the spectator system. For the $\bar{p} \to D^0$ transition we have the Fourier transform

$$
\int \frac{d^4z_2}{(2\pi)^4} e^{i\bar{k}_2 z_2} \langle D^0 : q' | \mathscr{T} \, \Phi^{S[ud]\dagger}_{a_2}(+z_2/2) \overline{\Psi}^c_{a_2'\alpha_2'}(-z_2/2) | \bar{p} : q, \nu \rangle \,, \tag{12}
$$

which can be interpreted in an analogous way as (11). The $p\bar{p} \to \overline{D^0}D^0$ amplitude (10) is thus a convolution of a hard scattering kernel with hadronic matrix elements Fourier transformed w.r.t. the average momenta $\bar{k}_1$ and $\bar{k}_2$ of the active partons.

For the active partons we can now introduce the momentum fractions

$$
x_1 := \frac{k_1^+}{p^+} \qquad \text{and} \qquad x_1' := \frac{k_1'^+}{p'^+} \,. \tag{13}
$$

For later convenience we also introduce the average fraction

$$
\bar{x}_1 = \frac{k_1^+ + k_1'^+}{p^+ + p'^+} = \frac{\bar{k}_1^+}{\bar{p}^+} \,, \tag{14}
$$

which is related to x_1 and x_1' by

$$x_1 = \frac{\bar{x_1}+\xi}{1+\xi} \qquad \text{and} \qquad x_1' = \frac{\bar{x_1}-\xi}{1-\xi}\,, \tag{15}$$

respectively.

As for the processes in Refs. [1] and [9], due to the large intrinsic scale given by the heavy quark mass m_c, the transverse and minus (plus) components of the active (anti-)parton momenta in the hard scattering kernel $\tilde{H}$ are small as compared to their plus (minus) components. Thus the parton momenta can be replaced by vectors lying in the scattering plane formed by the parent hadron momenta. For this assertion one only has to make the physically plausible assumptions that the momenta are almost on mass-shell and that their intrinsic transverse components (divided by the respective momentum fractions (15)) are smaller than a typical hadronic scale of the order of 1 GeV. We thus make the following replacements:

$$\begin{aligned}
k_1 &\to \left[k_1^+, \frac{x_1^2\boldsymbol{\Delta}_\perp^2}{8k_1^+}, -x_1\frac{\boldsymbol{\Delta}_\perp}{2}\right] \quad \text{with} \quad k_1^+ = x_1 p^+\,,\\
k_1' &\to \left[k_1'^+, \frac{m_c^2+x_1'^2\boldsymbol{\Delta}_\perp^2/4}{2k_1'^+}, x_1'\frac{\boldsymbol{\Delta}_\perp}{2}\right] \quad \text{with} \quad k_1'^+ = x_1' p'^+\,,\\
k_2 &\to \left[\frac{x_2^2\boldsymbol{\Delta}_\perp^2}{8k_2^-}, k_2^-, \quad x_2\frac{\boldsymbol{\Delta}_\perp}{2}\right] \quad \text{with} \quad k_2^- = x_2 q^-\,,\\
k_2' &\to \left[\frac{m_c^2+x_2'^2\boldsymbol{\Delta}_\perp^2/4}{2k_2'^-}, k_2'^-, -x_2'\frac{\boldsymbol{\Delta}_\perp}{2}\right] \quad \text{with} \quad k_2'^- = x_2' q'^-\,.
\end{aligned} \tag{16}$$

As a consequence of these replacements it is then possible to explicitely perform the integrations over $\bar{k}_1^-$, $\bar{k}_2^+$, $\bar{\mathbf{k}}_{\perp 1}$ and $\bar{\mathbf{k}}_{\perp 2}$. Furthermore the relative distance between the (anti-)$S[ud]$-diquark and the (anti-)c-quark field operators in the hadronic matrix elements is forced to be light-like, i.e. they have to lie on the light cone and thus the time ordering of the field operators can be dropped. After these simplifications one arrives at the following expression for the $p\bar{p} \to \overline{D^0}D^0$ amplitude:

$$\begin{aligned}
M_{\mu\nu} = \sum_{\mathrm{a}_\mathrm{i}^{(\prime)},\,\alpha_\mathrm{i}^{(\prime)}} &\int d\bar{k}_1^+\,\theta(\bar{k}_1^+)\int\frac{dz_1^-}{2\pi}e^{i\bar{k}_1^+ z_1^-}\int d\bar{k}_2^-\,\theta(\bar{k}_2^-)\int\frac{dz_2^+}{2\pi}e^{i\bar{k}_2^- z_2^+}\\
&\times\langle\overline{D^0}:p'|\Psi^c_{a_1'\alpha_1'}(-\bar{z}_1/2)\Phi^{S[ud]}_{a_1}(+\bar{z}_1/2)|p:p,\mu\rangle\,\tilde{H}_{a_i^{(\prime)}\alpha_i'}\left(\bar{k}_1,\bar{k}_2\right)\\
&\times\langle D^0:q'|\Phi^{S[ud]\dagger}_{a_2}(+\bar{z}_2/2)\overline{\Psi}^c_{a_2'\alpha_2'}(-\bar{z}_2/2)|\bar{p}:q,\nu\rangle\,.
\end{aligned} \tag{17}$$

From now on we will omit the color and spinor labels whenever this does not lead to ambiguities and replace the field-operator arguments $\bar{z}_1$ and $\bar{z}_2$ by their non-vanishing components z_1^- and z_2^+, respectively. Furthermore, if one uses $\bar{k}_1^+ = \bar{x}_1\bar{p}^+$ and $\bar{k}_2^- = \bar{x}_2\bar{q}^-$ to rewrite the $\bar{k}_1^+$ and $\bar{k}_2^-$

integrations in the amplitude (17) as integrations over the longitudinal momentum fractions $\bar{x_1}$ and $\bar{x_2}$, respectively, one arrives at,

$$\begin{aligned} M_{\mu\nu} = & \int d\bar{x}_1\, \bar{p}^+ \int \frac{dz_1^-}{2\pi} e^{i\bar{x}_1 \bar{p}^+ z_1^-} \int d\bar{x}_2\, \bar{q}^- \int \frac{dz_2^+}{2\pi} e^{i\bar{x}_2 \bar{q}^- z_2^+} \\ & \times \langle \overline{D^0} : p' | \Psi^c(-z_1^-/2) \Phi^{S[ud]}(+z_1^-/2) | p : p, \mu \rangle \, \tilde{H}\left(\bar{x}_1 \bar{p}^+, \bar{x}_2 \bar{q}^-\right) \\ & \times \langle D^0 : q' | \Phi^{S[ud]\dagger}(+z_2^+/2) \overline{\Psi}^c(-z_2^+/2) | \bar{p} : q, \nu \rangle \,. \end{aligned} \tag{18}$$

As in [1] for $p \to \Lambda_c^+$ ($\bar{p} \to \overline{\Lambda}_c^-$), the $p \to \overline{D^0}$ ($\bar{p} \to D^0$) transition matrix element is expected to exhibit a pronounced peak w.r.t. the momentum fraction. The position of the peak is approximately at

$$x_0 = \frac{m_c}{M} = 0.68\,. \tag{19}$$

From Eq. (9) one then infers that the relevant average momentum fractions $\bar{x_1}$ and $\bar{x_2}$ have to be larger than the skewness ξ. This means that the convolution integrals in (18) have to be performed only from ξ to 1 and not from 0 to 1.

In the following section we will analyze the soft hadronic matrix elements in some more detail.

4 Hadronic Transition Matrix Elements

Compared to (10) the Fourier transforms of the hadronic matrix elements for the $p \to \overline{D^0}$ and $\bar{p} \to D^0$ transitions are rendered to Fourier integrals solely over z_1^- and z_2^+, respectively. Hence we have to study the integral

$$\bar{p}^+ \int \frac{dz_1^-}{2\pi} e^{i\bar{x}_1 \bar{p}^+ z_1^-} \langle \overline{D^0} : p' | \Psi^c(-z_1^-/2) \Phi^{S[ud]}(+z_1^-/2) | p : p, \mu \rangle \tag{20}$$

over the $p \to \overline{D^0}$ transition matrix element and the integral

$$\bar{q}^- \int \frac{dz_2^+}{2\pi} e^{i\bar{x}_2 \bar{q}^- z_2^+} \langle D^0 : q' | \Phi^{S[ud]\dagger}(+z_2^+/2) \overline{\Psi}^c(-z_2^+/2) | \bar{p} : q, \nu \rangle \tag{21}$$

over the $\bar{p} \to D^0$ transition matrix element instead of (11) and (12), respectively.

We will first concentrate on the $p \to \overline{D^0}$ transition (20) and investigate the product of field operators $\Psi^c(-z_1^-/2)\Phi^{S[ud]}(+z_1^-/2)$. For this purpose we consider the $c-$quark field operator Ψ^c in the hadron frame of the outgoing $\overline{D^0}$, cf. e.g. [10, 11], where the $\overline{D^0}$ has no transverse momentum component. It can be reached from our symmetric CMS by a transverse boost [12, 13] with the boost parameters

$$b^+ = (1-\xi)\,\bar{p}^+ \quad \text{and} \quad \mathbf{b}_\perp = \frac{\boldsymbol{\Delta}_\perp}{2}\,. \tag{22}$$

In this hadron-out frame we write the field operator in terms of its "good" and "bad" LC components,

$$\Psi^c = \frac{1}{2}(\gamma^-\gamma^+ + \gamma^+\gamma^-)\,\Psi^c \equiv \Psi^c_+ + \Psi^c_-\,, \tag{23}$$

by means of the "good" and "bad" projection operators $\mathscr{P}^+ = \frac{1}{2}\gamma^-\gamma^+$ and $\mathscr{P}^- = \frac{1}{2}\gamma^+\gamma^-$, respectively. After doing that we eliminate the γ^- appearing in $\mathscr{P}^+$ and $\mathscr{P}^-$ by using the $\bar{c}-$quark energy projector

$$\sum_{\lambda_1'} v(k_1',\lambda_1')\bar{v}(k_1',\lambda_1') = k_1'\cdot\gamma - m_c\,. \tag{24}$$

In the hadron-out frame it explicitely takes on the form

$$\sum_{\lambda_1'} v(\hat{k}_1',\lambda_1')\bar{v}(\hat{k}_1',\lambda_1') = k_1'^+\gamma^- + \frac{m_c^2}{2k_1'^+}\gamma^+ - m_c\,, \tag{25}$$

since there the $\bar{c}-$quark momentum is

$$\hat{k}_1' = \left[k_1'^+, \frac{m_c^2}{2k_1'^+}, \mathbf{0}_\perp\right]. \tag{26}$$

With those replacements the $c-$quark field operator becomes

$$\begin{aligned}\Psi^c &= \frac{1}{2k_1'^+}\sum_{\lambda_1'}\Big\{v(\hat{k}_1',\lambda_1')\left(\bar{v}(\hat{k}_1',\lambda_1')\gamma^+\Psi^c\right)\\ &+ \gamma^+\Big[v(\hat{k}_1',\lambda')(\bar{v}(\hat{k}_1',\lambda_1')\Psi^c) + 2m_c\Psi^c\Big]\Big\}.\end{aligned} \tag{27}$$

As in the case of $p\bar{p}\to\Lambda_c^+\overline{\Lambda}_c^-$ in Ref. [1] one can argue that the contribution coming from $\left(\bar{v}(\hat{k}_1',\lambda_1')\gamma^+\Psi^c\right)$ dominates over the one in the square brackets and thus the latter one can be neglected. Since this dominant contribution can be considered as a plus component of a four-vector, one can immediately boost back to our symmetric CMS where it then still holds that

$$\Psi^c(-z_1/2) = \frac{1}{2k_1'^+}\sum_{\lambda_1'} v(k_1',\lambda_1')\left(\bar{v}(k_1',\lambda_1')\gamma^+\Psi^c(-z_1/2)\right). \tag{28}$$

Furthermore, one can even show that in $\left(\bar{v}(k_1',\lambda_1')\gamma^+\Psi^c(-z_1^-/2)\right)$ on the r.h.s. of (28) only the "good" component of $\Psi^c(-z_1^-/2)$ is projected out, since

$$\bar{v}(k_1',\lambda_1')\gamma^+\Psi^c(-z_1^-/2) = \bar{v}(k_1',\lambda_1')\gamma^+\mathscr{P}^+\Psi^c(-z_1^-/2)\,. \tag{29}$$

Finally we note that such manipulations are not necessary for the scalar field operator $\Phi^{S[ud]}$ of the $S[ud]-$diquark.

Putting everything together gives for the $p \to \overline{D^0}$ transition matrix element (20)

$$\bar{p}^+ \int \frac{dz_1^-}{2\pi} e^{i\bar{x}_1 \bar{p}^+ z_1^-} \langle \bar{D^0} : p' | \Psi^c(-z_1^-/2) \Phi^{S[ud]}(+z_1^-/2) | p : p, \mu \rangle =$$
$$\frac{\bar{p}^+}{2k_1'^+} \sum_{\lambda_1'} \int \frac{dz_1^-}{2\pi} e^{i\bar{x}_1 \bar{p}^+ z_1^-} \langle \bar{D^0} : p' | \nu\left(k_1', \lambda_1'\right) \left(\bar{\nu}(k_1', \lambda_1') \gamma^+ \Psi_+^c(-z_1^-/2) \right) \Phi^{S[ud]}(+z_1^-/2) | p : p, \mu \rangle \,. \tag{30}$$

Proceeding in an analogous way for the $\bar{p} \to D^0$ transition matrix element, where the role of the $+$ and $-$ components are interchanged, we get for (21)

$$\bar{q}^- \int \frac{dz_2^+}{2\pi} e^{i\bar{x}_2 \bar{q}^- z_2^+} \langle D^0 : q' | \Phi^{S[ud]\dagger}(+z_2^+/2) \overline{\Psi}^c(-z_2^+/2) | \bar{p} : q, \nu \rangle =$$
$$\frac{\bar{q}^-}{2k_2'^-} \sum_{\lambda_2'} \int \frac{dz_2^+}{2\pi} e^{i\bar{x}_2 \bar{q}^- z_2^+} \langle D^0 : q' | \Phi^{S[ud]\dagger}(+z_2^+/2) \left(\overline{\Psi}_+^c(-z_2^+/2) \gamma^- u\left(k_2', \lambda_2'\right) \right) \bar{u}\left(k_2', \lambda_2'\right) | \bar{p} : q, \nu \rangle \,. \tag{31}$$

Also here only the good components of the quark field are projected out on the r.h.s..

Using now (30) and (31) and attaching the spinors $v(k_1', \lambda_1')$ and $\bar{u}(k_2', \lambda_2')$ to the hard subprocess amplitude $\tilde{H}$ by introducing

$$H_{\lambda_1', \lambda_2'}(\bar{x}_1, \bar{x}_2) := \bar{u}\left(k_2', \lambda_2'\right) \tilde{H}\left(\bar{x}_1 \bar{p}^+, \bar{x}_2 \bar{q}^-\right) v\left(k_1', \lambda_1'\right) , \tag{32}$$

we get for the $p\bar{p} \to \overline{D^0} D^0$ amplitude (18),

$$\begin{aligned} M_{\mu\nu} = & \frac{1}{4(\bar{p}^+)^2} \sum_{\lambda_1', \lambda_2'} \int d\bar{x}_1 \int d\bar{x}_2 \, H_{\lambda_1', \lambda_2'}(\bar{x}_1, \bar{x}_2) \, \frac{1}{\bar{x}_1 - \xi} \, \frac{1}{\bar{x}_2 - \xi} \\ & \times \bar{v}(k_1', \lambda_1') \gamma^+ \quad \bar{p}^+ \int \frac{dz_1^-}{2\pi} \, e^{i\bar{x}_1 \bar{p}^+ z_1^-} \, \langle \bar{D^0} : p' | \Psi_+^c(-z_1^-/2) \Phi^{S[ud]}(+z_1^-/2) | p : p, \mu \rangle \\ & \times \bar{q}^- \int \frac{dz_2^+}{2\pi} \, e^{i\bar{x}_2 \bar{q}^- z_2^+} \, \langle D^0 : q' | \Phi^{S[ud]\dagger}(+z_2^+/2) \overline{\Psi}_+^c(-z_2^+/2) | \bar{p} : q, \nu \rangle \quad \gamma^- u\left(k_2', \lambda_2'\right) . \end{aligned} \tag{33}$$

Introducing the abbreviations

$$\mathscr{H}^{\bar{c}S}_{\lambda_1' \mu} := \bar{v}(k_1', \lambda_1') \gamma^+ \, \bar{p}^+ \int \frac{dz_1^-}{2\pi} \, e^{i\bar{x}_1 \bar{p}^+ z_1^-} \, \langle \bar{D^0} : p' | \Psi_+^c(-z_1^-/2) \Phi^{S[ud]}(+z_1^-/2) | p : p, \mu \rangle \tag{34}$$

and

$$\mathscr{H}^{c\bar{S}}_{\lambda_2' \nu} := \bar{q}^- \int \frac{dz_2^+}{2\pi} \, e^{i\bar{x}_2 \bar{q}^- z_2^+} \, \langle D^0 : q' | \Phi^{S[ud]\dagger}(+z_2^+/2) \overline{\Psi}_+^c(-z_2^+/2) | \bar{p} : q, \nu \rangle \, \gamma^- u\left(k_2', \lambda_2'\right) \tag{35}$$

for the pertinent projections of the hadronic transition matrix elements, we can write the hadronic scattering amplitude in a more compact form,

$$M_{\mu\nu} = \frac{1}{4(\bar{p}^+)^2} \sum_{\lambda_1', \lambda_2'} \int d\bar{x}_1 \int d\bar{x}_2 \, H_{\lambda_1', \lambda_2'}(\bar{x}_1, \bar{x}_2) \, \frac{1}{\bar{x}_1 - \xi} \, \frac{1}{\bar{x}_2 - \xi} \, \mathscr{H}^{\bar{c}S}_{\lambda_1' \mu} \, \mathscr{H}^{c\bar{S}}_{\lambda_2' \nu} . \tag{36}$$

5 Overlap Representation of $\mathscr{H}^{\bar{c}S}_{\lambda_1'\mu}$

In the following section we will derive a representation for the hadronic $p \to \overline{D^0}$ and $\bar{p} \to D^0$ transition matrix elements as an overlap of hadronic light cone-wave functions (LCWFs) for the valence Fock components of p and $\overline{D^0}$ [6]. Since we only need them for $\bar{x} > \xi$, i.e. in the DGLAP region, the hadronic transition matrix elements admit such a representation. For doing that we will make use of the Fock expansion of the hadron states and the Fourier decomposition of the partonic field operators in light cone QFT.

At a given light cone time, say $z^+ = 0$, the "good" independent dynamical field components $\Phi^{S[ud]}$ and $\Psi^c_+\left(-z_1^-/2\right)$ of the $S[ud]-$diquark and the $c-$quark, respectively, have the Fourier decomposition

$$\begin{aligned}\Phi^{S[ud]}\left(+z_1^-/2\right) = \int \frac{dk_1^+}{k_1^+} \int \frac{d^2k_{1\perp}}{16\pi^3}\,\theta\left(k_1^+\right) \Big[& a\left(S[ud] : k_1^+, \mathbf{k}_{1\perp}\right) e^{-\imath k_1^+ \frac{z_1^-}{2}} \\ & + b^\dagger\left(S[ud] : k_1^+, \mathbf{k}_{1\perp}\right) e^{+\imath k_1^+ \frac{z_1^-}{2}} \Big]\end{aligned} \tag{37}$$

and

$$\begin{aligned}\Psi^c_+\left(-z_1^-/2\right) = \int \frac{dk_1'^+}{k_1'^+} \int \frac{d^2k'_{1\perp}}{16\pi^3}\,\theta\left(k_1'^+\right) \sum_{\lambda_1'} \Big[& c\left(c : k_1'^+, \mathbf{k}'_{1\perp}, \lambda_1'\right) u_+\left(k_1', \lambda_1'\right) e^{+\imath k_1'^+ \frac{z_1^-}{2}} \\ & + d^\dagger\left(c : k_1'^+, \mathbf{k}'_{1\perp}, \lambda_1'\right) v_+\left(k_1', \lambda_1'\right) e^{-\imath k_1'^+ \frac{z_1^-}{2}} \Big] .\end{aligned} \tag{38}$$

The spinors u_+ and v_+ are the "good" components of the (anti-)quark spinors u and v, i.e., $u_+ = \mathscr{P}^+ u$ and $v_+ = \mathscr{P}^+ v$. The operators a and $b^\dagger$ are the annihilator of an $S[ud]$-diquark and the creator of an $\overline{S[ud]}$-diquark, respectively. The operator c annihilates a c-quark and the operator $d^\dagger$ creates a $\bar{c}$-quark. Their action on the vacuum gives the single-parton states

$$a^\dagger\left(S[ud] : k_1^+, \mathbf{k}_{1\perp}\right) | 0 \rangle = | S[ud] : k_1^+, \mathbf{k}_{1\perp} \rangle , \tag{39}$$

$$b^\dagger\left(S[ud] : k_1^+, \mathbf{k}_{1\perp}\right) | 0 \rangle = | \overline{S[ud]} : k_1^+, \mathbf{k}_{1\perp} \rangle , \tag{40}$$

$$c^\dagger\left(c : k_1'^+, \mathbf{k}'_{1\perp}, \lambda_1'\right) | 0 \rangle = | c : k_1'^+, \mathbf{k}'_{1\perp}, \lambda_1' \rangle , \tag{41}$$

$$d^\dagger\left(c : k_1'^+, \mathbf{k}'_{1\perp}, \lambda_1'\right) | 0 \rangle = | \bar{c} : k_1'^+, \mathbf{k}'_{1\perp}, \lambda_1' \rangle , \tag{42}$$

which are normalized as follows

$$\langle \cdots : k'^+, \mathbf{k}'_\perp, \lambda' \,|\, \cdots : k^+, \mathbf{k}_\perp, \lambda \rangle = 16\pi^3 k^+ \,\delta\left(k'^+ - k^+\right) \delta^{(2)}\left(\mathbf{k}'_\perp - \mathbf{k}_\perp\right) \delta_{\lambda',\lambda} . \tag{43}$$

In the case of $S[ud]$ states no $\lambda^{(\prime)}$ and no $\delta_{\lambda',\lambda}$ appear. This normalization is in accordance with the (anti-)commutation relations

$$\begin{aligned}\left[a\left(S[ud] : k'^+, \mathbf{k}'_\perp\right), a^\dagger\left(S[ud] : k^+, \mathbf{k}_\perp\right)\right] &= \left[b\left(S[ud] : k'^+, \mathbf{k}'_\perp\right), b^\dagger\left(S[ud] : k^+, \mathbf{k}_\perp\right)\right] \\ &= 16\pi^3 k^+ \,\delta\left(k'^+ - k^+\right) \delta^{(2)}\left(\mathbf{k}'_\perp - \mathbf{k}_\perp\right)\end{aligned} \tag{44}$$

and

$$\begin{aligned}\{c\left(c:k'^{+},\mathbf{k}'_{\perp},\lambda'\right),c^{\dagger}\left(c:k^{+},\mathbf{k}_{\perp},\lambda\right)\} &= \{d\left(c:k'^{+},\mathbf{k}'_{\perp},\lambda'\right),d^{\dagger}\left(c:k^{+},\mathbf{k}_{\perp},\lambda\right)\}\\ &= 16\pi^{3}k^{+}\,\delta\left(k'^{+}-k^{+}\right)\delta^{(2)}\left(\mathbf{k}'_{\perp}-\mathbf{k}_{\perp}\right)\delta_{\lambda',\lambda}\,.\end{aligned} \tag{45}$$

In the Fock state decomposition hadrons on the light front are replaced by a superposition of parton states. Taking only into account the valence Fock state, the proton- and the $\overline{D^0}$-state in our quark-diquark picture are represented as

$$\begin{aligned}|\,p:p,\mu\rangle = \int d\tilde{x}\,\frac{d^{2}\tilde{k}_{\perp}}{16\pi^{3}}\,\psi_{p}\left(\tilde{x},\tilde{\mathbf{k}}_{\perp}\right)\,\frac{1}{\sqrt{\tilde{x}(1-\tilde{x})}}\\ \times|\,S_{[ud]}:\tilde{x}p^{+},\tilde{\mathbf{k}}_{\perp}+\tilde{x}\mathbf{p}_{\perp}\rangle\,|\,u:(1-\tilde{x})p^{+},-\tilde{\mathbf{k}}_{\perp}+(1-\tilde{x})\mathbf{p}_{\perp},\mu\rangle\end{aligned} \tag{46}$$

and

$$\begin{aligned}|\,\overline{D^0}:p'\rangle = \int d\hat{x}'\,\frac{d^{2}\hat{k}'_{\perp}}{16\pi^{3}}\,\psi_{D}\left(\hat{x}',\hat{\mathbf{k}}'_{\perp}\right)\,\frac{1}{\sqrt{\hat{x}'(1-\hat{x}')}}\,\frac{1}{\sqrt{2}}\sum_{\lambda'}\left(2\lambda'\right)\\ \times|\,\bar{c}:\hat{x}'p'^{+},\hat{\mathbf{k}}'_{\perp}+\hat{x}'\mathbf{p}'_{\perp},\lambda'\rangle\,|\,u:(1-\hat{x}')p'^{+},-\hat{\mathbf{k}}'_{\perp}+(1-\hat{x}')\mathbf{p}'_{\perp},-\lambda'\rangle\,,\end{aligned} \tag{47}$$

respectively, with normalization

$$\langle\cdots:p'^{+},\mathbf{p}'_{\perp}(,\lambda')\,|\cdots:p^{+},\mathbf{p}_{\perp}(,\lambda)\rangle = 16\pi^{3}p^{+}\,\delta\left(p'^{+}-p^{+}\right)\delta^{(2)}\left(\mathbf{p}'_{\perp}-\mathbf{p}_{\perp}\right)\left(\delta_{\lambda',\lambda}\right)\,. \tag{48}$$

Also here, in the case of the pseudoscalar D^0 and $\overline{D^0}$ states no $\lambda^{(\prime)}$ and no $\delta_{\lambda',\lambda}$ appear. ψ_p and ψ_D are the LCWFs of the proton and the $\overline{D^0}$, respectively, which will be specified in Sec. 7. The LCWFs do not depend on the total momentum of the hadron, but only on the momentum coordinates of the partons relative to the hadron momentum. Those relative momenta are most easily identified in the hadron-frame of the parent hadron. Here we have assumed that the partons inside the proton and the $\overline{D^0}$ have zero orbital angular momentum. The arguments of the light cone-wave functions are related to the average momenta and momentum fractions by:

$$\tilde{x}_1 = \frac{\bar{x}_1+\xi}{1+\xi}\,,\quad \tilde{\boldsymbol{k}}_{1\perp} = \bar{\boldsymbol{k}}_{1\perp}-\frac{1-\bar{x}_1}{1+\xi}\frac{\boldsymbol{\Delta}_{\perp}}{2}\,, \tag{49}$$

$$\tilde{x}_2 = \frac{\bar{x}_2}{1+\xi}\,,\quad \tilde{\boldsymbol{k}}_{2\perp} = \bar{\boldsymbol{k}}_{2\perp}+\frac{\bar{x}_2}{1+\xi}\frac{\boldsymbol{\Delta}_{\perp}}{2}\,, \tag{50}$$

$$\hat{x}'_1 = \frac{\bar{x}_1-\xi}{1-\xi}\,,\quad \hat{\boldsymbol{k}}'_{1\perp} = \bar{\boldsymbol{k}}_{1\perp}+\frac{1-\bar{x}_1}{1-\xi}\frac{\boldsymbol{\Delta}_{\perp}}{2}\,, \tag{51}$$

$$\hat{x}'_2 = \frac{\bar{x}_2}{1-\xi}\,,\quad \hat{\boldsymbol{k}}'_{2\perp} = \bar{\boldsymbol{k}}_{2\perp}-\frac{\bar{x}_2}{1-\xi}\frac{\boldsymbol{\Delta}_{\perp}}{2}\,. \tag{52}$$

Using the expressions above, we can write the hadronic matrix elements appearing in (33) as

$$\begin{aligned}\mathscr{H}^{\bar{c}S}_{\lambda'_1\mu} = -\sqrt{2}\mu\bar{p}^{+}\int\frac{d\bar{x}d^{2}\bar{k}_{\perp}}{16\pi^{3}}\sqrt{\frac{\bar{x}-\xi}{\bar{x}+\xi}}\,\psi_{D}\left(\hat{x}'(\bar{x},\xi),\hat{\mathbf{k}}'_{\perp}(\bar{\mathbf{k}}_{\perp},\bar{x},\xi)\right)\\ \times\,\psi_{p}\left(\tilde{x}(\bar{x},\xi),\tilde{\mathbf{k}}_{\perp}(\bar{\mathbf{k}}_{\perp},\bar{x},\xi)\right)\,\delta\left(\bar{x}_1-\bar{x}\right)\delta_{-\lambda'_1,\mu}\end{aligned} \tag{53}$$

for the $p \to \overline{D^0}$ transition and

$$\begin{aligned}\mathscr{H}^{c\bar{S}}_{\lambda_2'\mu} = &-\sqrt{2}v\bar{q}^- \int \frac{d\bar{y}d^2\bar{l}_\perp}{16\pi^3}\sqrt{\frac{\bar{y}-\xi}{\bar{y}+\xi}}\,\psi_D\left(\hat{y}'(\bar{y},\xi),\hat{\mathbf{l}}'_\perp(\bar{\mathbf{l}}_\perp,\bar{y},\xi)\right)\\ &\times\psi_p\left(\tilde{y}(\bar{y},\xi),\tilde{\mathbf{l}}_\perp(\bar{\mathbf{l}}_\perp,\bar{y},\xi)\right)\delta\left(\bar{x}_2-\bar{y}\right)\delta_{-\lambda_2',v}\end{aligned} \tag{54}$$

for the $\bar{p} \to D^0$ transition. Here we have used that

$$\bar{v}\left(k_1',\lambda_1'\right)\gamma^+ v\left(k_1',-\mu\right) = 2k_1'^+ \quad \text{and} \quad \bar{u}\left(k_2',-v\right)\gamma^- u\left(k_2',\lambda_2'\right) = 2k_2'^- . \tag{55}$$

Collecting all pieces we finally get

$$\begin{aligned}M_{\mu v} = &\frac{\mu v}{2}\int d\bar{x}_1\int d\bar{x}_2\, H_{-\mu,-v}(\bar{x}_1,\bar{x}_2)\,\frac{1}{\sqrt{\bar{x}_1^2-\xi^2}}\frac{1}{\sqrt{\bar{x}_2^2-\xi^2}}\\ &\times\int\frac{d^2\bar{k}_\perp}{16\pi^3}\,\psi_D\left(\hat{x}'(\bar{x}_1,\xi),\hat{\mathbf{k}}'_\perp(\bar{\mathbf{k}}_\perp,\bar{x}_1,\xi)\right)\psi_p\left(\tilde{x}(\bar{x}_1,\xi),\tilde{\mathbf{k}}_\perp(\bar{\mathbf{k}}_\perp,\bar{x}_1,\xi)\right)\\ &\times\int\frac{d^2\bar{l}_\perp}{16\pi^3}\,\psi_D\left(\hat{y}'(\bar{x}_2,\xi),\hat{\mathbf{l}}'_\perp(\bar{\mathbf{l}}_\perp,\bar{x}_2,\xi)\right)\psi_p\left(\tilde{y}(\bar{x}_2,\xi),\tilde{\mathbf{l}}_\perp(\bar{\mathbf{l}}_\perp,\bar{x}_2,\xi)\right).\end{aligned} \tag{56}$$

Furthermore, we can take advantage of the expected shape of the $p \to \overline{D^0}$ ($\bar{p} \to D^0$) transition matrix elements. Due to their pronounced peak around x_0 only kinematical regions in the hard scattering amplitude close to the peak position are enhanced by the hadronic transition matrix elements. For the hard partonic subprocess we therefore apply a "peaking approximation" i.e. we replace the momentum fractions appearing in the hard-scattering amplitude by x_0. Then the hard scattering amplitude can be pulled out of the convolution integral and the $p\bar{p} \to \overline{D^0}D^0$ amplitude simplifies further to

$$\begin{aligned}M_{\mu v} = &\frac{\mu v}{2}H_{-\mu,-v}(x_0,x_0)\,\Big[\int_\xi^1 d\bar{x}\,\frac{1}{\sqrt{\bar{x}^2-\xi^2}}\int\frac{d^2\bar{k}_\perp}{16\pi^3}\\ &\psi_D\left(\hat{x}'(\bar{x},\xi),\hat{\mathbf{k}}'_\perp(\bar{\mathbf{k}}_\perp,\bar{x},\xi)\right)\psi_p\left(\tilde{x}(\bar{x},\xi),\tilde{\mathbf{k}}_\perp(\bar{\mathbf{k}}_\perp,\bar{x},\xi)\right)\Big]^2,\end{aligned} \tag{57}$$

where the term in square bracket can be considered as a sort of generalized form factor.

6 Hard Scattering Subprocess

Before we start to specify the LCWFs occuring in this overlap representation of the $p \to \overline{D^0}$ ($\bar{p} \to D^0$) transition, we will first calculate scattering amplitudes of the hard partonic $S[ud]\overline{S[ud]} \to \bar{c}c$ subprocess within the peaking approximation.

The hard-scattering amplitudes for the hard partonic subprocess, as shown in Fig. 3, is given by

$$H_{\lambda_1',\lambda_2'} = \imath\frac{4}{9}\left(-\imath g_s\bar{u}\left(k_2',\lambda_2'\right)\gamma^\mu v\left(k_1',\lambda_1'\right)\right)\frac{-\imath g_{\mu v}}{\left(k_1+k_2\right)^2}\left(\left(-\imath g_s F_s\right)\left(k_1-k_2\right)^v\right). \tag{58}$$

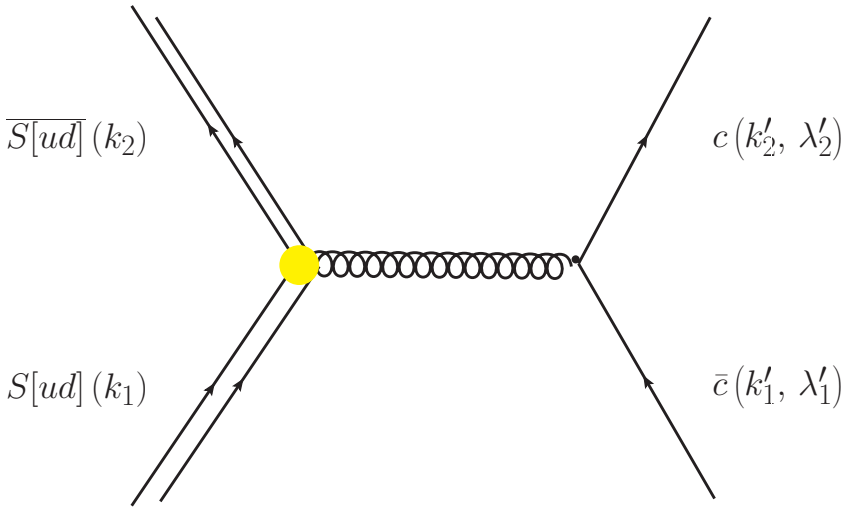

Figure 3: The hard scattering process on the partonic level $S[ud]\overline{S[ud]} \to c\bar{c}$.

$4/9$ is the color factor which we have attached to the hard-scattering amplitude. $g_s = \sqrt{4\pi\alpha_s}$ is the "usual" strong coupling constant and F_s denotes the diquark form factor at the gluon-diquark vertex. This diquark form factor takes care of the composite nature of the $S[ud]$-diquark and the fact that for large s the diquark should dissolve into quarks. We have taken the phenomenological form factor from Ref. [14], namely

$$F_s(\hat{s}) = \left| \frac{Q_0^2}{Q_0^2 - \hat{s}} \right|, \quad Q_0^2 = 3.22\,\mathrm{GeV}^2, \quad \hat{s} > Q_0^2. \tag{59}$$

It is just the analytic continuation of a space-like form factor to the time-like region. The original space-like form factor was introduced in Ref. [15] (where it has been obtained from fits to the structure functions of deep inelastic lepton-hadron scattering, to the electromagnetic proton form factor and elastic proton-proton data at large momentum transfer). It should be remarked here that such a continuation is not unique, the form factor can acquire unknown phases when doing the continuation. But fortunately such phases are irrelevant w.r.t. the physics, which is the reason for taking the absolute value in (59).

With the help of the peaking approximation we can express the subprocess amplitudes in terms of the kinematical variables of the full process. For the different helicity combinations

we explicitely have,

$$\begin{aligned} H_{++} &= +4\pi\alpha_s(x_0^2 s)\,F_s(x_0^2 s)\,\frac{4}{9}\,\frac{2M}{\sqrt{s}}\cos\theta\,, \\ H_{+-} &= -4\pi\alpha_s(x_0^2 s)\,F_s(x_0^2 s)\,\frac{4}{9}\,\sin\theta\,, \\ H_{-+} &= -4\pi\alpha_s(x_0^2 s)\,F_s(x_0^2 s)\,\frac{4}{9}\,\sin\theta\,, \\ H_{--} &= -4\pi\alpha_s(x_0^2 s)\,F_s(x_0^2 s)\,\frac{4}{9}\,\frac{2M}{\sqrt{s}}\cos\theta\,. \end{aligned} \tag{60}$$

7 Modelling the Hadronic Transition Matrix Elements

In order to make numerical predictions we have to specify the LCWFs for the proton and the D^0. We will use wave functions of the form

$$\psi \sim e^{-a^2\sum_i \frac{\mathbf{k}_{i\perp}^2+m_i^2}{x_i}}\,, \tag{61}$$

which can be traced back to a harmonic oscillator ansatz [17] that is transformed to the light cone [18]. In [19] it has been adapted to the case of baryons within a quark-diquark picture. According to [1, 16] we write the wave functions of a proton in an $S[ud]u$ Fock state as

$$\psi_p(x,\mathbf{k}_\perp) = N_p\,x\,e^{-a_p^2\frac{\mathbf{k}_\perp^2}{x(1-x)}} \tag{62}$$

and the one of a pseudoscalar D^0 meson in a $u\bar{c}$ Fock state as

$$\psi_D(x,\mathbf{k}_\perp) = N_D\,e^{-a_D^2 M^2\frac{(x-x_0)^2}{x(1-x)}}\,e^{-a_D^2\frac{\mathbf{k}_\perp^2}{x(1-x)}}\,. \tag{63}$$

Here x is the momentum fraction of the active constituent, the $S[ud]$-diquark or the $\bar{c}-$quark, respectively. The mass exponential in (63) generates the expected pronounced peak at $x \approx x_0$ and is a slightly modified version of the one given in [19].

In each of the wave functions, (62) and (63), we have two free parameters: on the one hand the transverse size parameter $a_{p/D}$ and, on the other hand, the normalization constant $N_{p/D}$. The parameters can be associated with the mean intrinsic transverse momentum squared $\langle\mathbf{k}_\perp^2\rangle_{p/D}$ of the active constituent inside its parent hadron and with the probability to find the hadron in the specific Fock state (or with the decay constant $f_{p/D}$ of the corresponding hadron). The probabilities and the intrinsic transverse momenta for the valence Fock states as given in (46) and (47) can be calculated as

$$P_{p/D} = \int dx \int \frac{d^2k_\perp}{16\pi^3}\mid\psi_{p/D}(x,\mathbf{k}_\perp)\mid^2 \tag{64}$$

and

$$\langle\mathbf{k}_\perp^2\rangle_{p/D} = \frac{1}{P_{p/D}}\int dx\int\frac{d^2k_\perp}{16\pi^3}\mathbf{k}_\perp^2\mid\psi_{p/D}(x,\mathbf{k}_\perp)\mid^2, \tag{65}$$

respectively. Inserting the wave functions (62) and (63) into (64) and (65) we obtain

$$P_p = \frac{N_p^2}{640\pi^2 a_p^2}, \qquad \langle \mathbf{k}_\perp^2 \rangle_p = \frac{2}{21 a_p^2} \tag{66}$$

and

$$P_D = \frac{N_D^2}{32\pi^2 a_D^2} I_{11}(a_D^2), \qquad \langle \mathbf{k}_\perp^2 \rangle_D = \frac{1}{2a_D^2} \frac{I_{22}(a_D^2)}{I_{11}(a_D^2)}, \tag{67}$$

where we have introduced the abbreviation

$$I_{nm}(a_D^2) := \int_0^1 dx x^n (1-x)^m \exp\left[-2a_D^2 M^2 \frac{(x-x_0)^2}{x(1-x)}\right]. \tag{68}$$

For the proton we use the same parameters as in [1] and [16]. We choose $a_p = 1.1\text{GeV}^{-1}$ for the oscillator parameter and $P_p = 0.5$ for the valence Fock state probability. Choosing $P_p = 0.5$ for the proton may appear rather large at first sight. As a bound state of two quarks a diquark embodies also gluons and sea quarks and thus effectively incorporates also higher Fock states. Therefore a larger probability than one would expect for a 3-quark valence Fock state and a larger transverse size of the quark-diquark state appear plausible. Choosing the parameter values as stated above we get for the proton

$$\sqrt{\langle \mathbf{k}_\perp^2 \rangle_p} = 280\,\text{MeV} \qquad \text{and} \qquad N_p = 61.818\,\text{GeV}^{-2}. \tag{69}$$

For the D-meson we fix the two parameters such that we get certain values for the valence Fock state probability P_D and the decay constant f_D. The decay constant f_D is defined by the relation

$$\langle 0 \mid \overline{\Psi}^\mu(0) \gamma^\mu \gamma_5 \Psi^c(0) \mid D^0 : p \rangle = \imath f_D p^\mu. \tag{70}$$

Taking the plus component and inserting the fields as given in Sec. 5 we get (omitting phases)

$$2\sqrt{6} \int dx \frac{d^2 k_\perp}{16\pi^3} \psi_D(x, \boldsymbol{k}_\perp) = f_D, \tag{71}$$

such that

$$N_D = \frac{16\pi^2 a_D^2 f_D}{2\sqrt{6} I_{11}(a_D^2/2)}. \tag{72}$$

As value for the decay constant we take the experimental value $f_D = 206$ MeV from Ref. [8], for the valence Fock state probability we choose $P_D = 0.9$. This amounts to $a_D = 0.864\text{GeV}^{-1}$. As values for the normalization constant and for the root mean square of the intrinsic transverse momentum of the active quark we then get

$$\sqrt{\langle \mathbf{k}_\perp^2 \rangle_D} = 383\,\text{MeV} \qquad \text{and} \qquad N_D = 55.202\,\text{GeV}^{-2}, \tag{73}$$

respectively.

Let us now turn to the issue of the error assesment w.r.t. the parameters. For the decay constant of the D^0-meson we take $f_D = 206 \pm 8.9$ MeV as stated in Ref. [8]. The valence Fock state probability of the D-meson P_D is varied between 0.8 and 1. We do not take into account the uncertainties of the parameters appearing in the proton LCWF. They are small compared to the ones of the D-meson LCWF since they have been determined from detailed studies of other processes. The influence of the parameter uncertainties on the cross sections are indicated by grey error bands in Figs. 5 and 6.

We now turn to the wave-function overlap as derived in Sec. 5. When taking the model wave functions (62) and (63) we explicitely get

$$\begin{aligned}
&\int \frac{d^2\bar{k}_\perp}{16\pi^3} \psi_D\left(\hat{x}'(\bar{x},\xi), \hat{\mathbf{k}}'_\perp(\bar{\mathbf{k}}_\perp,\bar{x},\xi)\right) \psi_p\left(\tilde{x}(\bar{x},\xi), \tilde{\mathbf{k}}_\perp(\bar{\mathbf{k}}_\perp,\bar{x},\xi)\right) = \\
&= \frac{N_p N_D}{16\pi^2} \frac{(\bar{x}+\xi)\left(\bar{x}^2-\xi^2\right)(1-\bar{x})}{(1+\xi)} \frac{1}{a_D^2(1-\xi)^2(\bar{x}+\xi)+a_p^2(1+\xi)^2(\bar{x}-\xi)} \\
&\times \exp\left[-a_D^2 M^2 \frac{(\bar{x}-\xi-x_0(1-\xi))^2}{(\bar{x}-\xi)(1-\bar{x})}\right] \exp\left[-\boldsymbol{\Delta}_\perp^2 \frac{a_D^2 a_p^2 (1-\bar{x})}{a_D^2(1-\xi)^2(\bar{x}+\xi)+a_p^2(1+\xi)^2(\bar{x}-\xi)}\right].
\end{aligned} \tag{74}$$

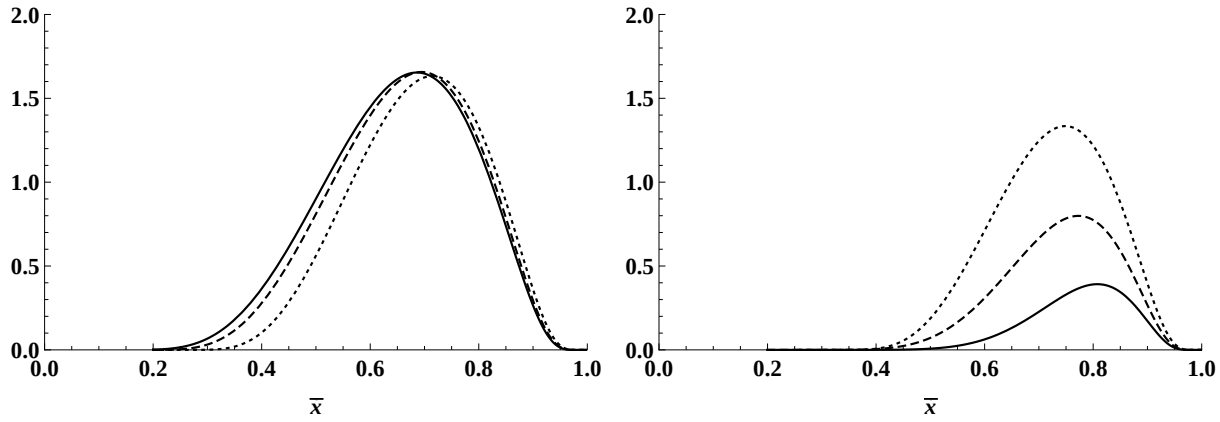

Figure 4: The wave-function overlap of Eq. (74) versus $\bar{x}$ at CMS scattering angle $\theta = 0$ (left figure) and $\theta = \pi/2$ (right figure). We show it for Mandelstam $s = 30$, 20 and 15 GeV^2 (solid, dashed and dotted curves).

In Fig. 4 we show the wave-function overlap of Eq. (74) versus the momentum fraction $\bar{x}$ with the parameters chosen as stated above. First we observe that it is centered at $\bar{x} \approx x_0$ for vanishing CMS scattering angle. Next let us compare the left and the right panel. We see that the magnitude of the wave-function overlap is strongly decreasing with increasing CMS scattering angle θ. The wave-function overlap is also more pronounced in magnitude and shape in forward direction. Furthermore, when comparing the overlap for different values of Mandelstam s, we observe that in the more important forward scattering hemisphere the overlap is increasing in

magnitude with increasing CMS energy s, whereas at large scattering angles this behavior is reversed.

8 Cross Sections

The differential cross section for $p\bar{p} \to \overline{D^0} D^0$ reads

$$\frac{d\sigma_{p\bar{p}\to\overline{D^0}D^0}}{d\Omega} = \frac{1}{4\pi} s \Lambda_M \Lambda_m \frac{d\sigma_{p\bar{p}\to\overline{D^0}D^0}}{dt} = \frac{1}{64\pi^2} \frac{1}{s} \frac{\Lambda_M}{\Lambda_m} \sigma_0 \,, \tag{75}$$

where we have introduced

$$\sigma_0 := \frac{1}{4} \sum_{\mu\nu} \mid M_{\mu\nu} \mid^2 \,. \tag{76}$$

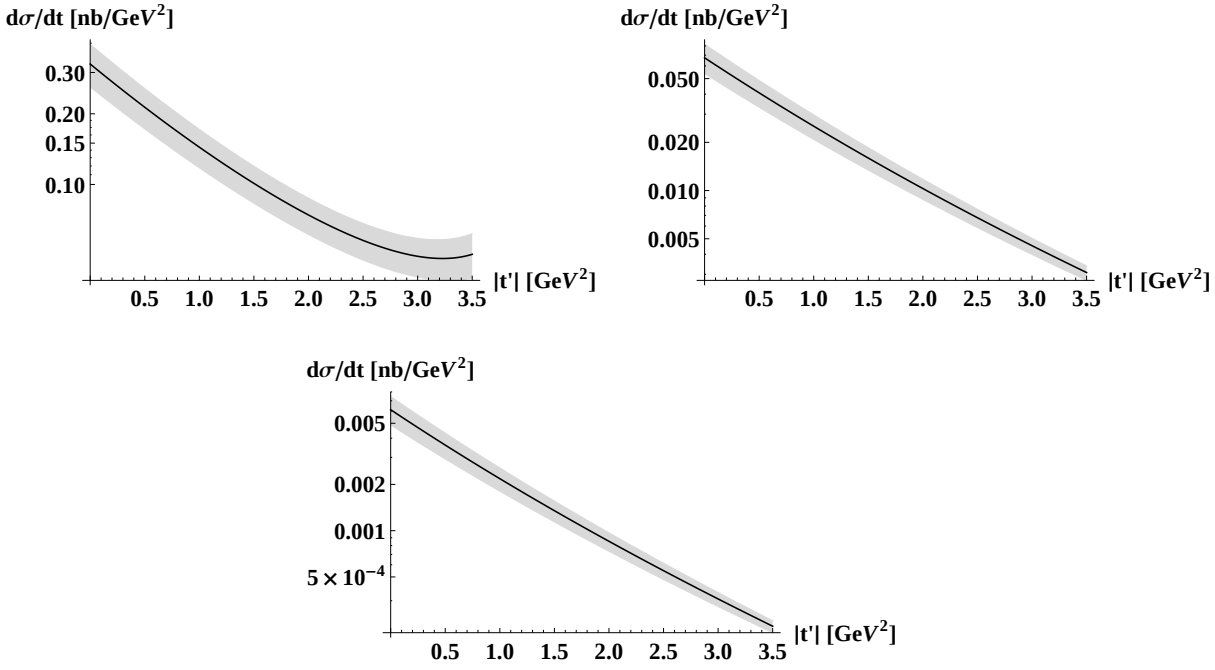

Figure 5: The differential cross section $d\sigma_{p\bar{p}\to\overline{D^0}D^0}/dt$ versus $\mid t' \mid$. On the upper left, upper right and lower panel we show it for Mandelstam $s = 15$, 20 and 30 GeV^2, respectively.

In Fig. 5 the differential cross section $d\sigma_{p\bar{p}\to\overline{D^0}D^0}/dt$ is plotted versus $\mid t' \mid$, again for Mandelstam $s = 15$, 20 and 30 GeV^2. The decrease of the cross section with increasing $\mid t' \mid$ can mainly be attributed to the wave-function overlap which gives rise to a generalized form factor (cf. Eq. (57)). This form factor enters the differential cross section to the fourth power. The forward direction is dominated by those amplitudes in which the helicities of the proton and antiproton (and also of the c and $\bar{c}$ quark) are equal. They go with $\cos\theta$. With increasing scattering

angle they compete with those in which proton and antiproton (and also c and $\bar{c}$) have opposite helicities. The latter go with $\sin\theta$ and dominate at 90°. If one looks at the energy dependence one observes that M_{++} and M_{--} are suppressed by a factor $2M/\sqrt{s}$ as compared to M_{+-} and M_{-+} (cf. Eq. (60)). This suppression is the reason that the cross section for $p\bar{p} \to \overline{D^0}D^0$ is smaller than the one for $p\bar{p} \to \Lambda_c^+\overline{\Lambda_c}^-$ in Ref. [1]. In the $p\bar{p} \to \Lambda_c^+\overline{\Lambda_c}^-$ case the factor $M/\sqrt{s}$ comes with those amplitudes which vanish in forward direction. When comparing the different panels of Fig. 5 one sees that the effect of the increase of the differential cross section with decreasing scattering angle becomes more pronounced for higher CMS energies.

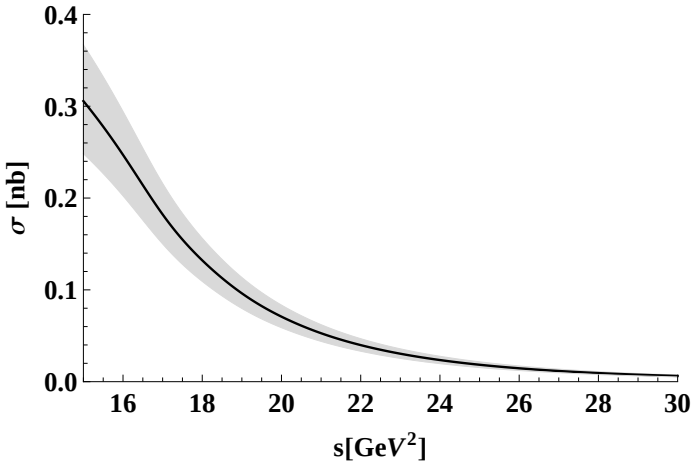

Figure 6: The integrated cross section $\sigma_{p\bar{p}\to\overline{D^0}D^0}$ versus Mandelstam s.

In Fig. 6 we show the integrated cross section σ versus Mandelstam s. It is of the order of 10^{-1} nb, which is one order of magnitude lower than the integrated cross section for $p\bar{p} \to \Lambda_c^+\overline{\Lambda_c}^-$ in Ref. [1]. This finding is in accordance with the diquark-model calculation of Ref. [16]. According to Ref. [16] larger cross sections (of the order of the $p\bar{p} \to \Lambda_c^+\overline{\Lambda_c}^-$ cross section) are to be expected for the $p\bar{p} \to D^+D^-$ reaction. This, however, requires to extend our handbag approach by including vector diquarks and will be the topic of future investigations. Our estimated cross section is about two orders of magnitude smaller than the predictions given in Refs. [20] and [21], where hadronic interaction models have been used. Whereas the authors of Ref. [20] determine their couplings of the initial proton to the intermediate and final charmed hadrons by means of QCD sum rules, the authors of Ref. [21] rather use SU(4) flavor symmetry. Though their predictions for the integrated $p\bar{p} \to \overline{D^0}D^0$ cross section are comparable, they differ substantially in the $p\bar{p} \to D^+D^-$ cross section which, in Ref. [20], is even smaller than our $p\bar{p} \to \overline{D^0}D^0$ cross section. Such big discrepancies reveal the high necessity of experimental data which allow to decipher between different dynamical models. Such experiments could also help to pin down the charm-quark content of the proton sea. A considerably higher cross section within our approach could only be explained if the charm-quark content of the proton sea was not negligible.

Acknowledgements

We acknowledge helpful discussions with L. Szymanowski. This work was supported by the Austrian Science Fund FWF under grant J 3163-N16 and via the Austrian-French scientific exchange program Amadeus.

Appendices

A Kinematics

The four-momentum transfer Δ can be written as (cf. (1), (2))

$$\Delta = \left[-2\xi \bar{p}^+ , \frac{M^2(1+\xi) - m^2(1-\xi) + \xi \boldsymbol{\Delta}_\perp^2/2}{2\bar{p}^+(1-\xi^2)} , \boldsymbol{\Delta}_\perp \right]. \tag{77}$$

Note that $\Delta^+ = -\Delta^-$ since $p' - p = q - q'$.

In order to find expressions for the sine and the cosine of the CMS scattering angle θ we write the absolute value of the three-momentum and the momentum component into z-direction of the incoming proton as

$$|\mathbf{p}| = \frac{\sqrt{s}}{2}\Lambda_m , \quad p_3 = \frac{\sqrt{s}}{2}\sqrt{\Lambda_m^2 - \boldsymbol{\Delta}_\perp^2/s} \tag{78}$$

and that of the outgoing $\bar{D}^0$ as

$$|\mathbf{p}'| = \frac{\sqrt{s}}{2}\Lambda_M , \quad |p_3'| = \frac{\sqrt{s}}{2}\sqrt{\Lambda_M^2 - \boldsymbol{\Delta}_\perp^2/s}, \tag{79}$$

respectively.

Note that we have chosen the coordinate system in such a way that the $\underline{z}$-component of the incoming proton momentum is always positive. But that of the outgoing D^0 can become negative at large scattering angles due to the unequal-mass kinematics. This change of sign occurs when $\boldsymbol{\Delta}_\perp^2$ reaches its maximal value

$$\boldsymbol{\Delta}_{\perp\max}^2 = s\Lambda_M^2 , \tag{80}$$

which follows directly from (79). Then the CMS scattering angle can be written as

$$\begin{aligned} \theta &= \arccos\left(\frac{p_3}{|\mathbf{p}|}\right) + \arccos\left(\frac{p_3'}{|\mathbf{p}'|}\right) \\ &= \arcsin\left(\frac{|\Delta_\perp|}{2|\mathbf{p}|}\right) + \arcsin\left(\frac{|\Delta_\perp|}{2|\mathbf{p}'|}\right) \qquad \text{for forward scattering} \\ &= \arcsin\left(\frac{|\Delta_\perp|}{2|\mathbf{p}|}\right) - \arcsin\left(\frac{|\Delta_\perp|}{2|\mathbf{p}'|}\right) + \pi \quad \text{for backward scattering.} \end{aligned} \tag{81}$$

Using (81) the sine and cosine of the CMS scattering angle θ turn out to be

$$\sin\theta = \sqrt{\frac{\boldsymbol{\Delta}_\perp^2}{s}}\frac{1}{\Lambda_m\Lambda_M}\left(\sqrt{\Lambda_m^2-\frac{\boldsymbol{\Delta}_\perp^2}{s}}+\mathrm{sign}\left(p_3'\right)\sqrt{\Lambda_m^2-\frac{\boldsymbol{\Delta}_\perp^2}{s}}\right) \tag{82}$$

and

$$\cos\theta = \frac{\mathrm{sign}\left(p_3'\right)}{\Lambda_m\Lambda_M}\left(\sqrt{\left(\Lambda_m^2-\frac{\boldsymbol{\Delta}_\perp^2}{s}\right)\left(\Lambda_M^2-\frac{\boldsymbol{\Delta}_\perp^2}{s}\right)}-\frac{1}{\mathrm{sign}\left(p_3'\right)}\frac{\boldsymbol{\Delta}_\perp^2}{s}\right), \tag{83}$$

respectively, where $\mathrm{sign}\left(p_3'\right)$ takes care of the kinematical situation of forward or backward scattering.

Now we are able to express several kinematical variables in a compact form. Starting from the definition (2) of the average hadron momentum $\bar{p}$ and using (78), (79), (82) and (83) its plus component can be written as

$$\begin{aligned}\bar{p}^+ &= \frac{1}{2}\left(p^+ + p'^+\right) = \frac{1}{2\sqrt{2}}\left((p_0+p_3)+\left(p_0'+p_3'\right)\right)\\ &= \frac{1}{4}\sqrt{\frac{s}{2}}\left[2+\sqrt{\Lambda_m^2-\boldsymbol{\Delta}_\perp^2/s}+\mathrm{sign}(p_3')\sqrt{\Lambda_M^2-\boldsymbol{\Delta}_\perp^2/s}\right]\\ &= \frac{1}{4}\sqrt{\frac{s}{2}}\left[2+\sqrt{\Lambda_m^2+\Lambda_M^2+2\Lambda_m\Lambda_M\cos\theta}\right].\end{aligned} \tag{84}$$

Note that in our symmetric CMS $\bar{q}^- = \bar{p}^+$. For the skewness parameter ξ we get

$$\begin{aligned}\xi &= \frac{p^+-p'^+}{p^++p'^+}\\ &= \frac{\sqrt{\Lambda_m^2-\boldsymbol{\Delta}_\perp^2/s}-\mathrm{sign}(p_3')\sqrt{\Lambda_M^2-\boldsymbol{\Delta}_\perp^2/s}}{2+\sqrt{\Lambda_m^2-\boldsymbol{\Delta}_\perp^2/s}+\mathrm{sign}(p_3')\sqrt{\Lambda_M^2-\boldsymbol{\Delta}_\perp^2/s}}\\ &= \frac{\Lambda_m^2-\Lambda_M^2}{\sqrt{\Lambda_m^2+\Lambda_M^2+2\Lambda_m\Lambda_M\cos\theta}}\,\frac{1}{2+\sqrt{\Lambda_m^2+\Lambda_M^2+2\Lambda_m\Lambda_M\cos\theta}}.\end{aligned} \tag{85}$$

Note that, as a consequence of the unequal-mass kinematics, ξ cannot become zero, which is different from, e.g., Compton scattering where ξ would be equal to zero in such a symmetric frame. For $p_3' \geq 0$, however, ξ is fairly small in our case and tends to zero for $s \to \infty$.

Now let us further investigate the Mandelstam variables and write them in a more compact form with the help of (78), (79), (82) and (83). Mandelstam t can be written as

$$\begin{aligned}t &= -\frac{\boldsymbol{\Delta}_\perp^2}{1-\xi^2}-\frac{2\xi}{1-\xi^2}\left[(1+\xi)M^2-(1-\xi)m^2\right]\\ &= -\frac{\boldsymbol{\Delta}_\perp^2}{2}-\frac{s}{4}\left[\Lambda_m^2+\Lambda_M^2-2\mathrm{sign}\left(p_3'\right)\sqrt{\Lambda_m^2-\boldsymbol{\Delta}_\perp^2/s}\sqrt{\Lambda_M^2-\boldsymbol{\Delta}_\perp^2/s}\right]\\ &= -\frac{s}{4}\left[\Lambda_m^2+\Lambda_M^2-2\Lambda_m\Lambda_M\cos\theta\right].\end{aligned} \tag{86}$$

It cannot become zero for forward scattering but acquires the value

$$t_0 \;:=\; t(\boldsymbol{\Delta}_\perp^2 = 0, p_3' \geq 0) \;=\; -\frac{s}{4}\,(\Lambda_m - \Lambda_M)^2\,, \tag{87}$$

and for backward scattering

$$t_1 \;:=\; t(\boldsymbol{\Delta}_\perp^2 = 0, p_3' \leq 0) \;=\; -\frac{s}{4}\,(\Lambda_m + \Lambda_M)^2\,. \tag{88}$$

It is furthermore convenient to introduce a "reduced" Mandelstam variable t' that vanishes for forward scattering,

$$\begin{aligned} t' \;&:= t - t_0 \\ &= -\frac{\boldsymbol{\Delta}_\perp^2}{2} - \frac{s}{2}\left[\Lambda_m\Lambda_M - \mathrm{sign}(p_3')\sqrt{\Lambda_m^2 - \boldsymbol{\Delta}_\perp^2/s}\sqrt{\Lambda_M^2 - \boldsymbol{\Delta}_\perp^2/s}\right] \\ &= -\frac{s}{2}\Lambda_m\Lambda_M\,(1-\cos\theta)\,. \end{aligned} \tag{89}$$

Also the transverse component of Δ can easily be written as a function of the sine and the cosine of the scattering angle θ using (82) and (83),

$$\boldsymbol{\Delta}_\perp^2 \;=\; s\frac{\Lambda_m^2\Lambda_M^2\sin^2\theta}{\Lambda_m^2 + \Lambda_M^2 + 2\Lambda_m\Lambda_M\cos\theta}\,, \tag{90}$$

or solving (89) for $\boldsymbol{\Delta}_\perp^2$ one finds

$$\boldsymbol{\Delta}_\perp^2 \;=\; -t'\frac{s\Lambda_m\Lambda_M + t'}{s/4(\Lambda_m+\Lambda_M)^2 + t'}. \tag{91}$$

If we define Mandelstam u for forward scattering in an analogous way

$$u_0 \;:= u\;(\boldsymbol{\Delta}_\perp^2 = 0, p_3' \geq 0) \;=\; -\frac{s}{4}\,(\Lambda_m + \Lambda_M)^2 \tag{92}$$

and for backward scattering

$$u_1 \;:=\; u(\boldsymbol{\Delta}_\perp^2 = 0, p_3' \leq 0) \;=\; -\frac{s}{4}\,(\Lambda_m - \Lambda_M)^2\,, \tag{93}$$

the sine and the cosine of half the CMS scattering angle θ can be written compactly as

$$\sin^2\left(\frac{\theta}{2}\right) \;=\; \frac{1-\cos\theta}{2} = \frac{t_0 - t}{s\Lambda_m\Lambda_M}\,, \tag{94}$$

$$\cos^2\left(\frac{\theta}{2}\right) \;=\; \frac{1+\cos\theta}{2} = \frac{u_1 - u}{s\Lambda_m\Lambda_M}\,, \tag{95}$$

respectively.

B Light Cone Spinors

For our purposes we use the light cone spinors [22, 23]. They read

$$u(p,\uparrow)=\frac{1}{2^{1/4}}\frac{1}{\sqrt{p^+}}\begin{pmatrix}p^+ + m/\sqrt{2}\\ p_\perp/\sqrt{2}\\ p^+ - m/\sqrt{2}\\ p_\perp/\sqrt{2}\end{pmatrix} \quad , \quad u(p,\downarrow)=\frac{1}{2^{1/4}}\frac{1}{\sqrt{p^+}}\begin{pmatrix}-p_\perp^*/\sqrt{2}\\ p^+ + m/\sqrt{2}\\ p_\perp^*/\sqrt{2}\\ -p^+ + m/\sqrt{2}\end{pmatrix}, \tag{96}$$

$$v(p,\uparrow)=\frac{-1}{2^{1/4}}\frac{1}{\sqrt{p^+}}\begin{pmatrix}-p_\perp^*/\sqrt{2}\\ p^+ - m/\sqrt{2}\\ p_\perp^*/\sqrt{2}\\ -p^+ - m/\sqrt{2}\end{pmatrix} \quad , \quad v(p,\downarrow)=\frac{-1}{2^{1/4}}\frac{1}{\sqrt{p^+}}\begin{pmatrix}p^+ - m/\sqrt{2}\\ p_\perp/\sqrt{2}\\ p^+ + m/\sqrt{2}\\ p_\perp/\sqrt{2}\end{pmatrix}. \tag{97}$$

for $p^3 > 0$ and

$$u(p,\uparrow)=\frac{1}{2^{1/4}}\frac{sign\left(p^1\right)}{\sqrt{p^-}}\begin{pmatrix}p_\perp^*/\sqrt{2}\\ p^- + m/\sqrt{2}\\ p_\perp^*/\sqrt{2}\\ p^- - m/\sqrt{2}\end{pmatrix} \quad , \quad u(p,\downarrow)=\frac{1}{2^{1/4}}\frac{-sign\left(p^1\right)}{\sqrt{p^-}}\begin{pmatrix}p^- + m/\sqrt{2}\\ -p_\perp/\sqrt{2}\\ -p^- + m/\sqrt{2}\\ p_\perp/\sqrt{2}\end{pmatrix}, \tag{98}$$

$$v(p,\uparrow)=\frac{1}{2^{1/4}}\frac{sign\left(p^1\right)}{\sqrt{p^-}}\begin{pmatrix}p^- - m/\sqrt{2}\\ -p_\perp/\sqrt{2}\\ -p^- - m/\sqrt{2}\\ p_\perp/\sqrt{2}\end{pmatrix} \quad , \quad v(p,\downarrow)=\frac{1}{2^{1/4}}\frac{-sign\left(p^1\right)}{\sqrt{p^-}}\begin{pmatrix}p_\perp^*/\sqrt{2}\\ p^- - m/\sqrt{2}\\ p_\perp^*/\sqrt{2}\\ p^- + m/\sqrt{2}\end{pmatrix} \tag{99}$$

for $p^3 < 0$. They satisfy the charge-conjugation relation

$$v(p,\lambda)=\imath\gamma^2 u^*(p,\lambda) \tag{100}$$

and are normalized as

$$\bar{u}_{\lambda'}(p)\,u_\lambda(p)=2m\delta_{\lambda'\lambda} \qquad \text{and} \qquad \bar{v}_{\lambda'}(p)\,v_\lambda(p)=-2m\delta_{\lambda'\lambda}. \tag{101}$$

C TDAs

Following Ref. [5] the $p\to\overline{D^0}$ transition matrix element can be decomposed at leading twist into the following covariant structures,

$$\begin{aligned}\tilde{\mathscr{H}}_\mu^{\bar{c}S} &:= \bar{p}^+\int\frac{dz_1^-}{2\pi}e^{\imath\bar{x}_1\bar{p}^+z_1^-}\left\langle\overline{D^0}:\,p'\mid\Psi_+^c\left(-z_1^-/2\right)\Phi^{S[ud]}\left(+z_1^-/2\right)\mid p:\,p,\mu\right\rangle\\ &=\gamma_5 u(p,\mu)V_1(\bar{x}_1,\xi,t)+\frac{\not{\Delta}}{M+m}\gamma_5 u(p,\mu)V_2(\bar{x}_1,\xi,t)\\ &\quad+u(p,\mu)\tilde{V}_1(\bar{x}_1,\xi,t)+\frac{\not{\Delta}}{M+m}u(p,\mu)\tilde{V}_2(\bar{x}_1,\xi,t),\end{aligned} \tag{102}$$

where we have introduced the $p \to \overline{D^0}$ TDAs $V_1, V_2, \tilde{V}_1$ and $\tilde{V}_2$. When evaluating the $p\bar{p} \to \overline{D^0} D^0$ amplitude the hadronic transition matrix element (102) appears within the spinor product

$$\mathscr{H}^{\bar{c}S}_{\lambda_1'\mu} = \bar{v}(k_1', \lambda_1')\, \gamma^+\, \tilde{\mathscr{H}}^{\bar{c}S}_{\mu}, \tag{103}$$

cf. (33). Expressed in terms of TDAs we thus have

$$\begin{aligned}
\mathscr{H}^{\bar{c}S}_{\lambda_1'\mu} =& \bar{v}(k_1', \lambda_1')\, \gamma^+ \gamma_5\, u(p,\mu)\, V_1(\bar{x}_1, \xi, t) + \bar{v}(k_1', \lambda_1')\, \gamma^+ \frac{\not{\Delta}}{M+m} \gamma_5\, u(p,\mu)\, V_2(\bar{x}_1, \xi, t) \\
&+ \bar{v}(k_1', \lambda_1')\, \gamma^+ u(p,\mu)\, \tilde{V}_1(\bar{x}_1, \xi, t) + \bar{v}(k_1', \lambda_1')\, \gamma^+ \frac{\not{\Delta}}{M+m}\, u(p,\mu)\, \tilde{V}_2(\bar{x}_1, \xi, t) \\
=& \sqrt{\frac{\bar{x}_1 - \xi}{1-\xi}} \Big[\bar{v}(p', \lambda_1')\, \gamma^+ \gamma_5\, u(p,\mu)\, V_1(\bar{x}_1, \xi, t) + \bar{v}(p', \lambda_1')\, \gamma^+ \frac{\not{\Delta}}{M+m} \gamma_5\, u(p,\mu)\, V_2(\bar{x}_1, \xi, t) \\
&+ \bar{v}(p', \lambda_1')\, \gamma^+ u(p,\mu)\, \tilde{V}_1(\bar{x}_1, \xi, t) + \bar{v}(p', \lambda_1')\, \gamma^+ \frac{\not{\Delta}}{M+m}\, u(p,\mu)\, \tilde{V}_2(\bar{x}_1, \xi, t) \Big],
\end{aligned} \tag{104}$$

after making the replacement $k_1' = x_1' p'$ in the $\bar{v}-$spinor. Evaluating the various spinor products which appear in (104) by using the light cone spinors of App. B gives

$$\mathscr{H}^{\bar{c}S}_{++} = \frac{4\bar{p}^+}{M+m} \sqrt{\frac{\bar{x}_1 - \xi}{1+\xi}} \frac{\Delta_\perp}{2} \left(V_2(\bar{x}_1, \xi, t) + \tilde{V}_2(\bar{x}_1, \xi, t) \right), \tag{105}$$

$$\mathscr{H}^{\bar{c}S}_{--} = \frac{4\bar{p}^+}{M+m} \sqrt{\frac{\bar{x}_1 - \xi}{1+\xi}} \frac{\Delta_\perp}{2} \left(V_2(\bar{x}_1, \xi, t) - \tilde{V}_2(\bar{x}_1, \xi, t) \right) \tag{106}$$

and

$$\begin{aligned}
\mathscr{H}^{\bar{c}S}_{+-} =& 2\bar{p}^+ \sqrt{\bar{x}_1 - \xi} \sqrt{1+\xi} \Big[V_1(\bar{x}_1, \xi, t) - \tilde{V}_1(\bar{x}_1, \xi, t) \\
&+ \frac{2\xi}{1+\xi} \frac{m}{M+m} \left(V_2(\bar{x}_1, \xi, t) + \tilde{V}_2(\bar{x}_1, \xi, t) \right) \Big],
\end{aligned} \tag{107}$$

$$\begin{aligned}
\mathscr{H}^{\bar{c}S}_{-+} =& -2\bar{p}^+ \sqrt{\bar{x}_1 - \xi} \sqrt{1+\xi} \Big[V_1(\bar{x}_1, \xi, t) + \tilde{V}_1(\bar{x}_1, \xi, t) \\
&+ \frac{2\xi}{1+\xi} \frac{m}{M+m} \left(V_2(\bar{x}_1, \xi, t) - \tilde{V}_2(\bar{x}_1, \xi, t) \right) \Big].
\end{aligned} \tag{108}$$

The TDAs $V_1, \tilde{V}_1, V_2$ and $\tilde{V}_2$ can now be expressed as linear combinations of $\mathscr{H}^{\bar{c}S}_{++}$, $\mathscr{H}^{\bar{c}S}_{--}$, $\mathscr{H}^{\bar{c}S}_{+-}$ and $\mathscr{H}^{\bar{c}S}_{-+}$. For our overlap representation of the hadronic transition matrix elements we have $\mathscr{H}^{\bar{c}S}_{++} = \mathscr{H}^{\bar{c}S}_{--} = 0$ (cf. Eq. (55)). This means that $V_2 = \tilde{V}_2 = 0$ and

$$V_1 = \frac{1}{4\bar{p}^+ \sqrt{\bar{x}_1 - \xi} \sqrt{1+\xi}} \left(\mathscr{H}^{\bar{c}S}_{+-} - \mathscr{H}^{\bar{c}S}_{-+}, \right), \tag{109}$$

$$\tilde{V}_1 = -\frac{1}{4\bar{p}^+\sqrt{\bar{x}_1-\xi}\sqrt{1+\xi}}\left(\mathscr{H}^{\bar{c}S}_{+-}+\mathscr{H}^{\bar{c}S}_{-+}\right). \tag{110}$$

We further have $\mathscr{H}^{\bar{c}S}_{+-} = -\mathscr{H}^{\bar{c}S}_{-+}$ (cf. Eq. (53)), so that we finally get

$$V_1 = \frac{1}{2\bar{p}^+\sqrt{\bar{x}_1-\xi}\sqrt{1+\xi}}\mathscr{H}^{\bar{c}S}_{+-} \quad \text{and} \quad \tilde{V}_1 = 0\,. \tag{111}$$

References

[1] A. T. Goritschnig, P. Kroll and W. Schweiger, Eur. Phys. J. A **42** (2009) 43 [arXiv:0905.2561 [hep-ph]].

[2] B. Pire and L. Szymanowski, Phys. Rev. D **71** (2005) 111501 [hep-ph/0411387] and Phys. Lett. B **622** (2005) 83.

[3] J. P. Lansberg, B. Pire, K. Semenov-Tian-Shansky and L. Szymanowski, arXiv:1210.0126 [hep-ph].

[4] M. F. M. Lutz *et al.* [PANDA Collaboration], arXiv:0903.3905 [hep-ex].

[5] B. Pire, K. Semenov-Tian-Shansky and L. Szymanowski, Phys. Rev. D **82**, 094030 (2010) and Phys. Rev. D **84**, 074014 (2011); J. P. Lansberg, B. Pire, K. Semenov-Tian-Shansky and L. Szymanowski, Phys. Rev. D **85**, 054021 (2012).

[6] M. Diehl, T. Feldmann, R. Jakob and P. Kroll, Nucl. Phys. B **596** (2001) 33 [Erratum-ibid. B **605** (2001) 647] [hep-ph/0009255]; S. J. Brodsky, M. Diehl and D. S. Hwang, Nucl. Phys. B **596**, 99 (2001).

[7] R. Jakob, P. Kroll, M. Schürmann and W. Schweiger, Z. Phys. A **347** (1993) 109 [hep-ph/9310227].

[8] J. Beringer *et al.* [Particle Data Group], Phys. Rev. D **86** (2012) 010001.

[9] M. Diehl, Th. Feldmann, R. Jakob and P. Kroll, Eur. Phys. J. C **8** (1999) 409 [arXiv:hep-ph/9811253].

[10] J. B. Kogut and D. E. Soper, Phys. Rev. D **1** (1970) 2901.

[11] S. J. Brodsky and G. P. Lepage, Adv. Ser. Direct. High Energy Phys. **5** (1989) 93.

[12] P. A. M. Dirac, Rev. Mod. Phys. **21** (1949) 392.

[13] H. Leutwyler and J. Stern, Annals Phys. **112** (1978) 94.

[14] P. Kroll, T. Pilsner, M. Schürmann and W. Schweiger, Phys. Lett. B **316** (1993) 546 [hep-ph/9305251].

[15] M. Anselmino, P. Kroll and B. Pire, Z. Phys. C **36** (1987) 89.

[16] P. Kroll, B. Quadder and W. Schweiger, Nucl. Phys. B **316** (1989) 373.

[17] M. Wirbel, B. Stech and M. Bauer, Z. Phys. C **29** (1985) 637.

[18] X. - H. Guo and T. Huang, Phys. Rev. D **43** (1991) 2931.

[19] J. G. Körner and P. Kroll, Phys. Lett. B **293** (1992) 201. J. G. Körner and P. Kroll, Z. Phys. C **57** (1993) 383.

[20] A. Khodjamirian, C. Klein, T. Mannel and Y. M. Wang, Eur. Phys. J. A **48**, 31 (2012).

[21] J. Haidenbauer and G. Krein, Few Body Syst. **50**, 183 (2011) [arXiv:1010.5324 [hep-ph]].

[22] D. E. Soper, Phys. Rev. D **5** (1972) 1956.

[23] S. J. Brodsky, H. C. Pauli and S. S. Pinsky, Phys. Rept. **301** (1998) 299 [arXiv:hep-ph/9705477].